TECHNICAL REPORT

WVT-6933

EXPERIMENTAL AND ANALYTICAL STRAINS IN AN EDGE-CRACKED SHEET

BY

JOHN H. UNDERWOOD

J. L. SWEDLOW

AND

DAVID P. KENDALL

SEPTEMBER 1969

BENET R&E LABORATORIES

WATERVLIET ARSENAL

WATERVLIET—NEW YORK

AMCMS No. 5011.11.85500

DA Project 1-T-0-61102-B32A

DISPOSITION

Destroy this report when it is no longer needed. Do not return it to the originator.

DISCLAIMER

The findings in this report are not to be construed as an official Department of the Army position.

WVT-6933

EXPERIMENTAL AND ANALYTICAL STRAINS IN AN EDGE-CRACKED SHEET

Technical Report

By

John H. Underwood

J. L. Swedlow*

David P. Kendall

*Department of Mechanical Engineering, Carnegie-Mellon University
Pittsburgh, Pennsylvania

EXPERIMENTAL AND ANALYTICAL STRAINS IN AN EDGE-CRACKED SHEET

Abstract

The nature and some details of the elasto-plastic strain distribution ahead of the crack tip in an edge-cracked sheet has been determined by experiment and analysis. The experiment uses the optical interference and moire techniques. The analysis is a generalized plane stress model using the finite element method; the measured uniaxial stress-strain properties of the materials are used as input to the analysis. Materials investigated by one or both methods are 1018 steel, copper, 90-10 and 70-30 brass, and 6061-T6 aluminum. Of these materials, meaningful comparisons between experiment and analysis have been made for those with no discontinuity in uniaxial behavior; copper, 90-10 brass, and aluminum. The agreement between experiment and analysis can be significantly affected by how well the early, uniaxial, yield properties used in the analysis represent the actual properties of the experimental specimens.

The main factors which control the general nature of crack-tip strain are (1) degree of strain hardening, shown by both experimental and analytical results and (2) thickness of the experimental specimen. For materials of low strain hardening and at relatively low loads, the measured crack-tip deformation tends to be three dimensional in character and restricted in extent to about one specimen thickness in the direction normal to the crack. For higher hardening and at higher loads, broader, two-dimensional strain distributions result with better correlation with analysis. Stress distributions from the analysis in the area ahead of the crack are also shown and tend to support the strain results.

Cross-Reference Data

Crack-tip Strain

Fracture Mechanics

Finite Elements

Optical Measurement

Strain Distribution

Strain Hardening

TABLE OF CONTENTS

TABLE OF CONTENTS

Figures (Continued)

INTRODUCTION

As part of continuing programs of research in the authors' respective institutions, experimental and analytical studies of strain in the vicinity of a crack have been performed independently. The results were then compared. The overall objective is to have the capability for predicting stresses and strains near a crack in a body under load. With this knowledge of crack-tip stress and strain states it should be possible to determine the conditions under which a crack will propagate to failure. This approach is useful for crack related fracture where the material properties and specimen geometry combine to produce significant plastic deformation around a crack. For this type of behavior, often referred to as large scale yielding, the plastically deformed area around the crack is large enough relative to specimen and crack dimensions so that linear elastic analyses do not apply.

Preliminary to detailed experimental and analytical studies of strains in the vicinity of a crack, the procedures must be developed for making precise measurements and performing accurate calculations. Initial efforts along these lines have been reported separately[1][2][3] for a study that involved commercially pure copper. The present paper reviews further efforts

SUMMARY OF PROCEDURES

Experimental crack-tip strain distributions and deformation patterns have been obtained from edge cracked sheet specimens of 70-30 brass, 90-10 brass, 6061-T6 aluminum, and 1018 steel, all of standard commercial quality. The specimen configuration and coordinate system used are shown in Figure 1. The experimental techniques are optical interference, used to obtain the

z direction strain data and deformation patterns, and moiré grid interference, used to obtain the y direction strain data. The optical interference technique is a single beam, proof plate system using a thalium vapor light source of 5350A wavelength, so that each interference fringe corresponds to about a 10 microinch z direction displacement. The moiré technique uses a 6000 line per inch grating ruled on the specimen and a 2000 line per inch transparent master grating. Further details of the strain measurement methods are given in earlier reports[1][2]. The general test method is also similar to that described in earlier work[2]. The specimens are notched and fatigue cracked; annealed to remove effects of deformation during fatigue cracking; polished and ruled; and then loaded in increments, with crack-tip data taken at several loads. The dimensions, annealing temperature, and yield properties of the specimens are shown in Table I. One exception to the experimental procedure is the lack of an annealing treatment following fatigue cracking for the aluminum specimens. Any effective anneal would also have modified the alloy to a condition no longer representative of any standard treatment. The maximum applied stress used for fatigue cracking the aluminum was 8800 psi compared with 15,000 psi, the lowest applied stress for the crack-tip strain data reported. Thus, we believe that the prior fatigue cracking had no major effect on the aluminum data reported here.

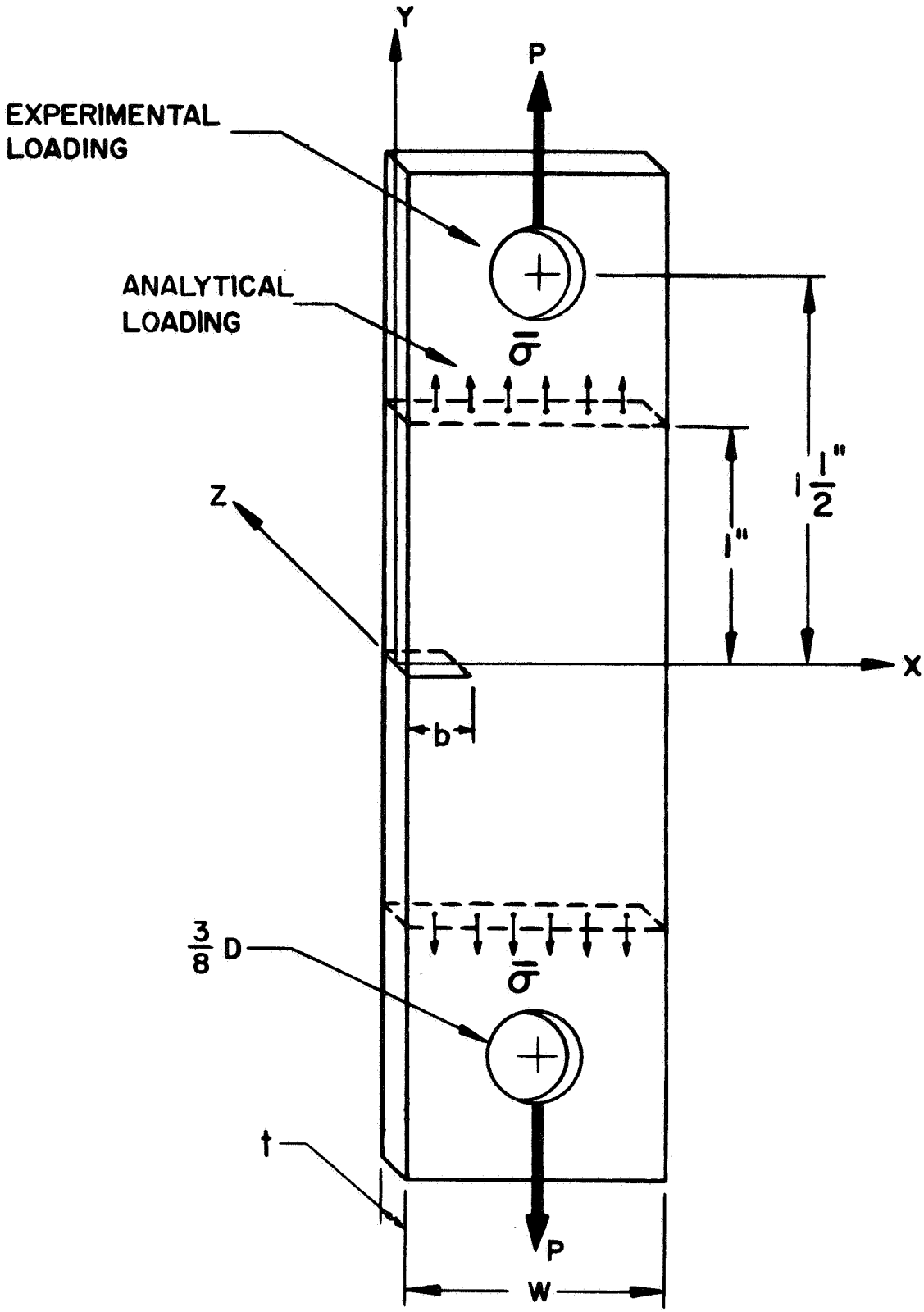

Figure 1. Specimen Configuration

TABLE I. TEST SPECIMENS

Specimen	Dimensions, inches w	t	b	Anneal	Prop. Limit psi	.1% Yield psi
90-10 Brass						
R-1	.99	.118	.27	900°F	9,350	12,500
R-5	.99	.036	.26			
70-30 Brass						
B-1	.98	.123	.25	900°F	16,100	17,200
B-11	.98	.040	.25			
6061-T6 Alum.						
Al-1	.98	.081	.28			
Al-3	.97	.032	.26	--	34,000	39,800
Al-5	.98	.052	.26			
1018 Steel						
S-6	.99	.114	.24	1600°F	---	38,000

The experimental specimen is loaded through 3/8 in. dia. holes located 1.5 widths above the crack as shown in Figure 1. To determine whether this type of loading produces the same stress field around the crack as the uniform loading in the analytical work, a photoelastic model of the specimen was tested. The results were compared with finite element results from the same crack geometry but with uniform stress applied along the line one width above the crack. These results are shown in Figure 2, as a plot of the principal stress difference versus distance across the specimen. Data are shown along the line ahead of the crack where most of the subsequent data are shown and along a line above the crack line where the value of the principal stress difference is higher. The agreement obtained in both cases indicates that elastic loading in the pin loaded specimen produces substantially the same crack-tip stress field as uniform elastic loading. Alternatively, it could be observed that the crack dominates other features of the geometry to the point where distinction between the two types of loading is not significant.

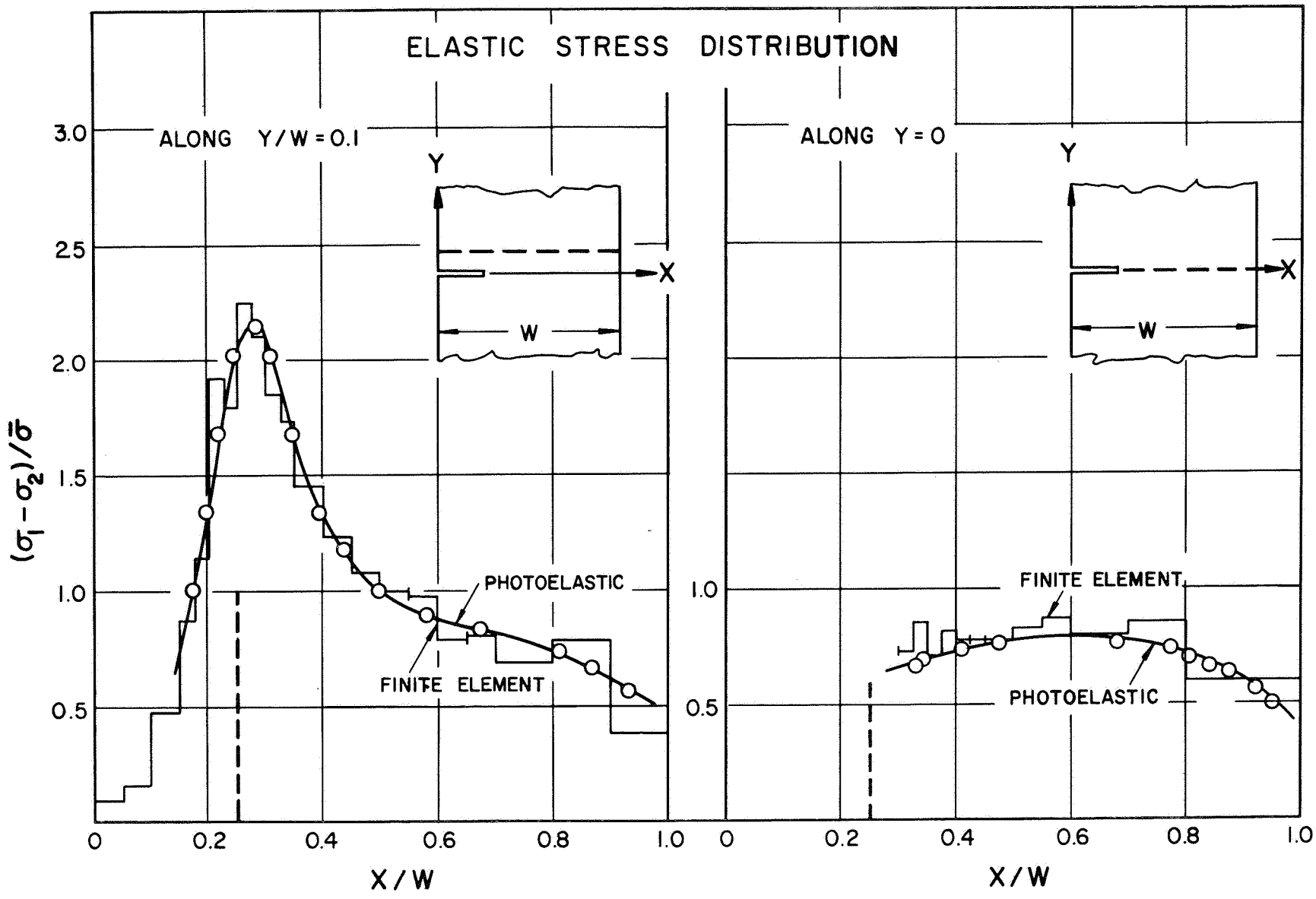

Figure 2. Elastic Stress Distribution

The analytical procedures derive from a general formulation[4]; in the present case generalized plane stress is employed. The material is presumed to yield according to the Mises criterion and work-hardening is incorporated. The numerical technique is the standard finite element method, modified to allow for elasto-plastic flow. Some details have been reported earlier[5], and are not repeated here. It is worth noting, however, that the computer program accepts as input the actual stress-strain curve of the material to be studied. Thus, the material behavior is incorporated directly into the analysis in as accurate a form as it may be obtained. This feature appears crucial to meaningful comparisons between experiment and analysis[3].

DISCUSSION OF EXPERIMENTAL RESULTS

Figure 3 shows representative crack-tip plastic deformation observed in 1018 steel, 70-30 brass, 90-10 brass, 6061-T6 aluminum. The specimens shown are S-6, B-1, R-1, Al-1 respectively. The interference photographs were taken after load removal, with the loads chosen to produce about the same overall size of deformation zone. The interference fringes outline the z direction displacement around the crack. They can also be interpreted as lines of constant z strain averaged through the sheet thickness. From this type of data we have characterized the crack-tip plastic deformation behavior of these materials as being a combination of two basic deformation modes, a through-thickness shear mode and an in-plane extensional mode.

The steel sample is a good example of the shear mode in which the plastic deformation occurs as shear deformation on a set of closely spaced planes inclined 45° to the plane of the sheet and parallel with the

x axis. Thus, the shear deformation is three-dimensional in nature. The geometry of the deformation requires that the total extent of the deformation area above and below the crack be slightly greater than t. This is confirmed by the steel results where the extent of the deformation zone above the crack only is about 0.7 t. The 90-10 brass specimen shows the in-plane deformation mode which appears to be two-dimensional in nature, i.e., no change in the deformation pattern through the thickness. The in-plane deformation is not restricted in extent by the specimen thickness, as can be seen by the extended deformation pattern in the 90-10 brass. The 70-30 brass and the aluminum show combinations of the two modes with the shear mode dominant in the 70-30 brass and the in-plane mode becoming dominant in the aluminum.

Based on the analysis of the results obtained thus far, it appears that crack-tip deformation in thin sheet depends to a large degree on certain features of the uniaxial deformation behavior. The uniaxial stress-strain properties of the four materials studied are shown in Figure 4. The characteristic of the uniaxial data which affects the crack-tip behavior to the greatest extent is the strain hardening exponent "n" corresponding to the early stages of yielding. This agrees with Gerberich's observation[6] in center-cracked sheet that strain hardening has a major influence on the nature of the plastic zone. Referring to Figures 3 and 4, the crack-tip deformation is nearly pure shear for the steel which has an initial hardening exponent near zero; for materials with higher initial "n" the in-plane mode becomes more prevalent. The abrupt transition from low to high "n" seen in the steel and the 70-30 brass also has an effect on the crack-tip deformation. It is possible that an early transition as in the 70-30 brass causes the

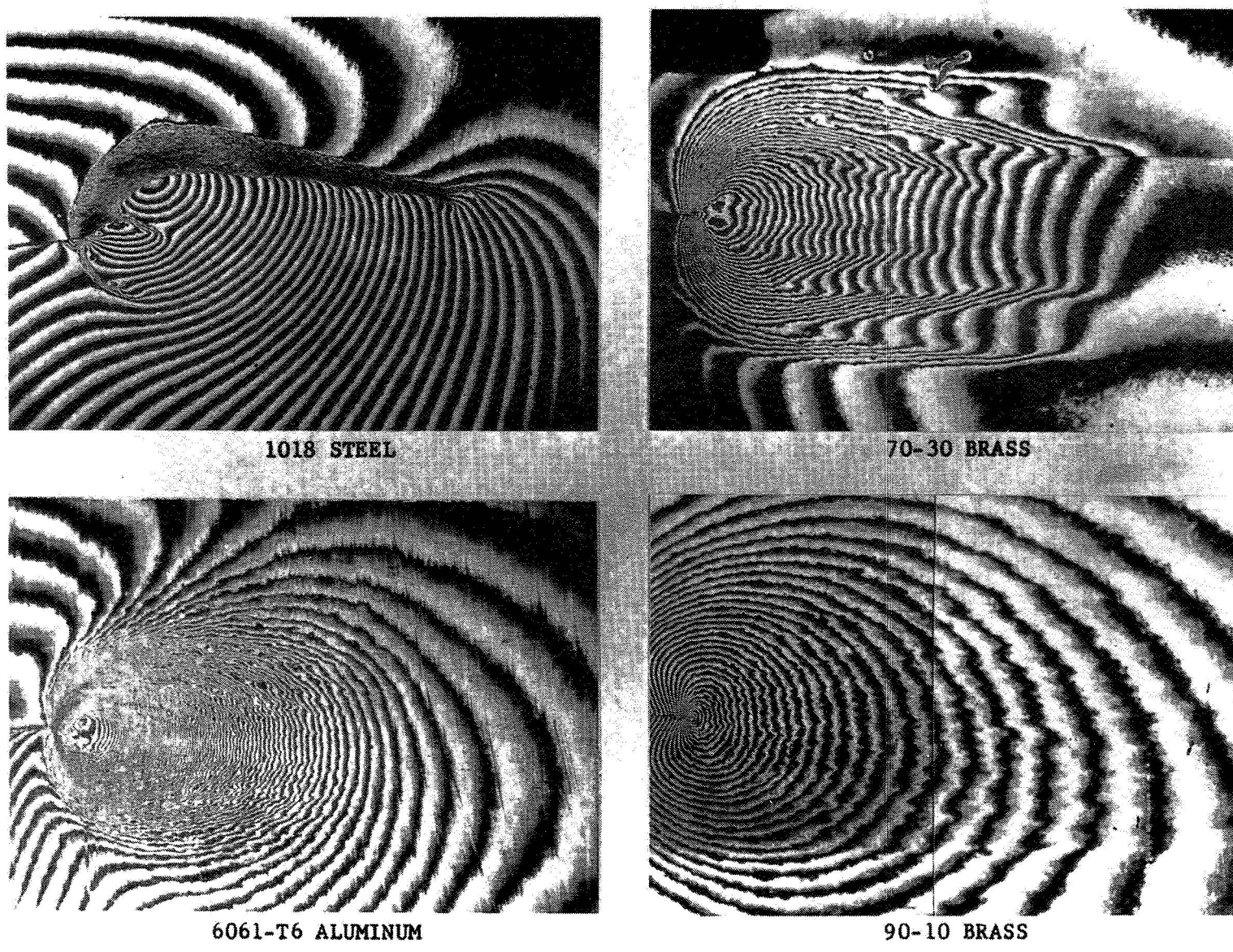

Figure 3. Interference Photographs

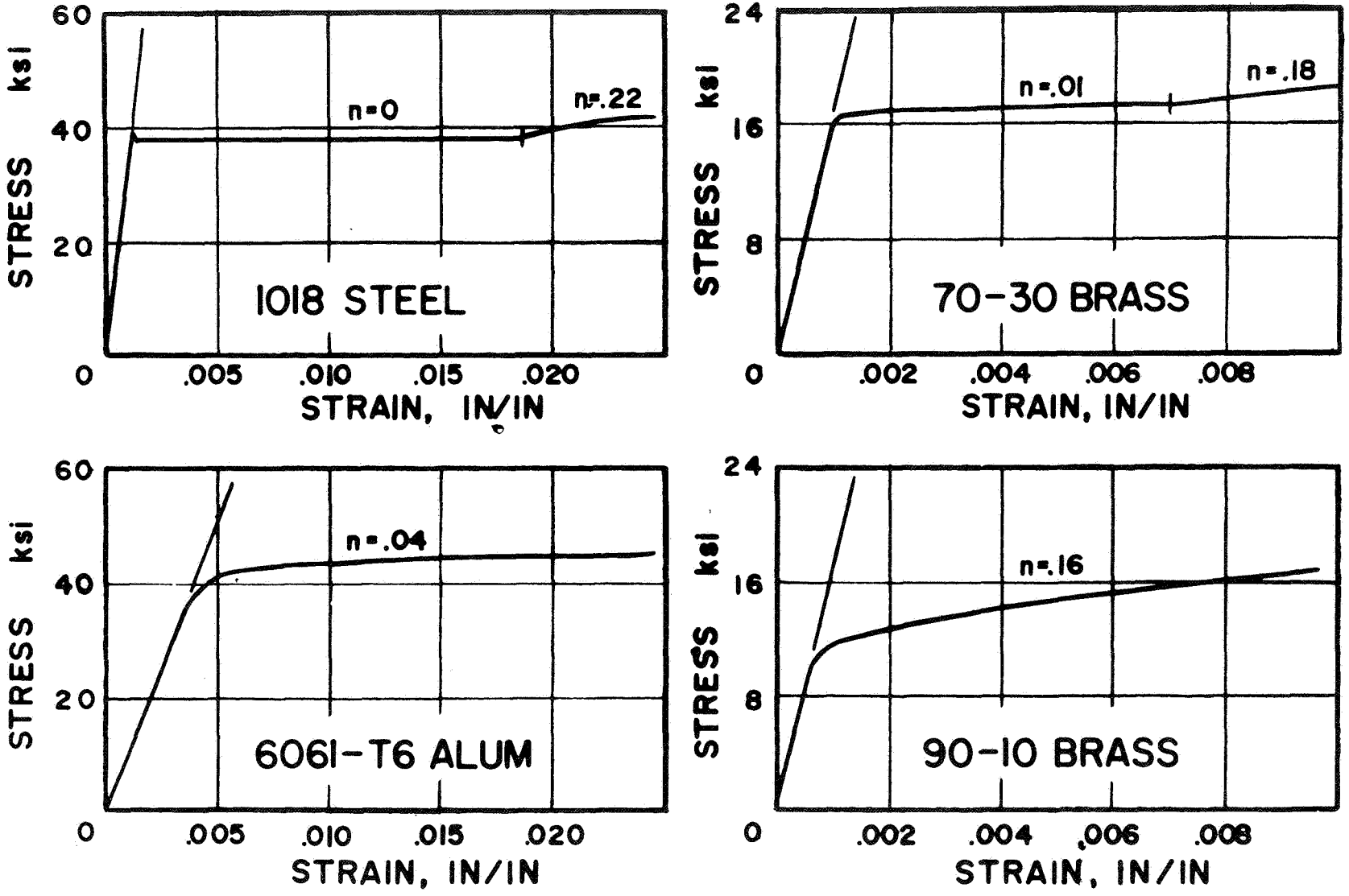

Figure 4. Uniaxial Stress-Strain Data

multi-fingered shear deformation observed in that material. The sharpness of yield of the uniaxial data seems to affect the crack-tip behavior only in how clearly defined the deformation zone appears as it forms, not in the shape and size of zone formed. Elastic modulus and yield stress have only secondary effects on the nature of the crack-tip behavior. The yield stress will of course affect the load level at which plastic deformation begins for a given specimen geometry.

The effects of material properties and specimen thickness on crack-tip behavior are shown in another way in Figure 5, which shows oblique lighting photographs of brass specimens. The 70-30 brass specimen, B-1, shows the thickness-related shear deformation while the 90-10 specimen, R-5, shows an in-plane deformation pattern. It should be noted that although the thickness of the 90-10 specimen is less than one-third that of the 70-30 specimen, it nevertheless shows a broader deformation pattern.

Figure 6 shows after-load interference photographs from 70-30 brass specimen B-11. The deformation patterns could be explained by a transition from predominantly shear deformation at low load with a deformation zone about equal in size to t to the larger in-plane deformation pattern at high load. This transition in crack-tip behavior corresponds to the change in hardening exponent in 70-30 brass from $n = 0.01$ at low strain to $n = 0.18$ at high strain, i.e., above 0.007 in/in (see Figure 4). This explanation is supported by the results in that for the low load, with a z direction strain of about 0.004 ahead of the crack, a thickness related deformation zone is formed. At the intermediate load, with a strain of about 0.012, the original zone can still be seen but with additional deformation occurring outside the zone.

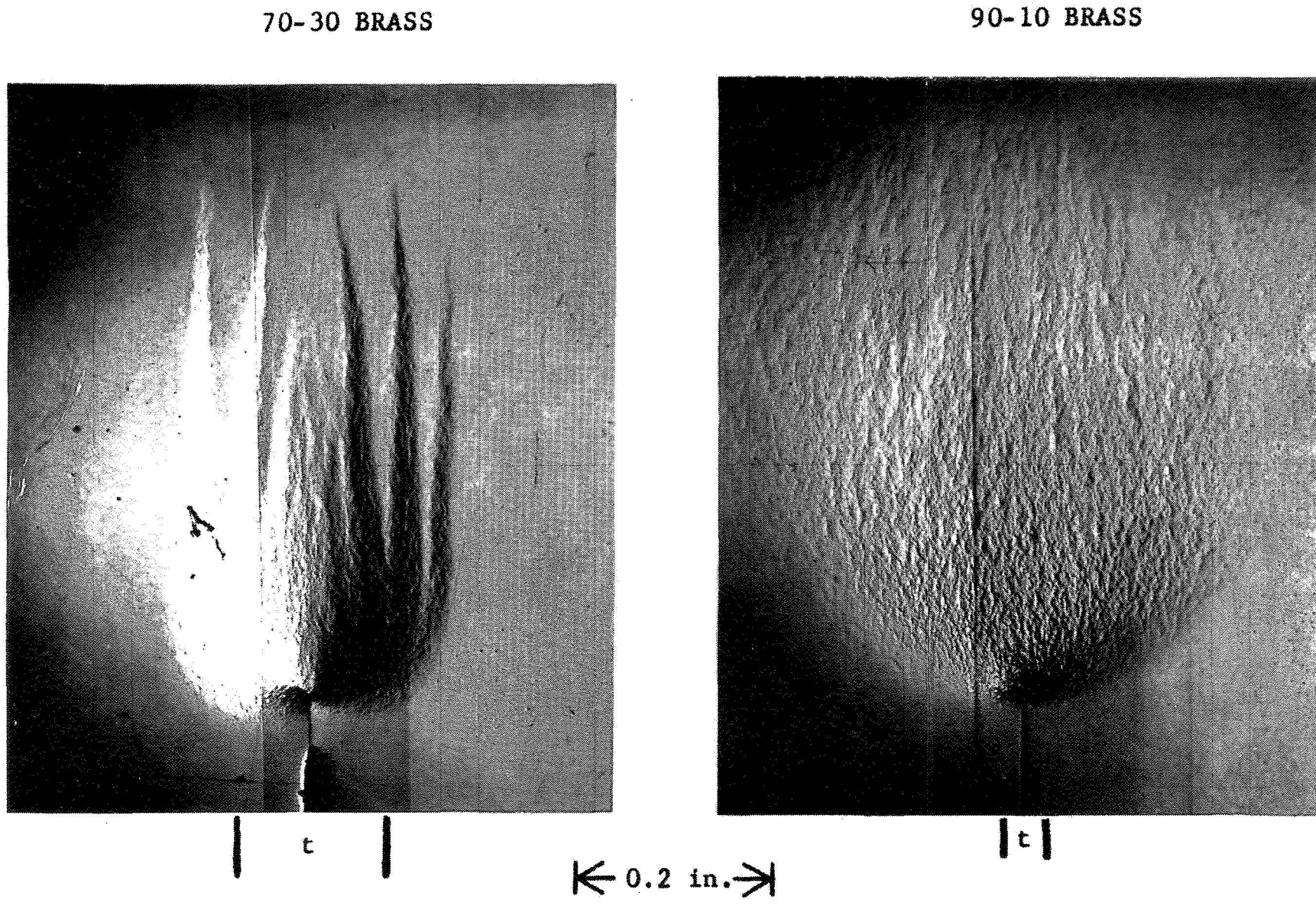

Figure 5. Oblique Light Photographs

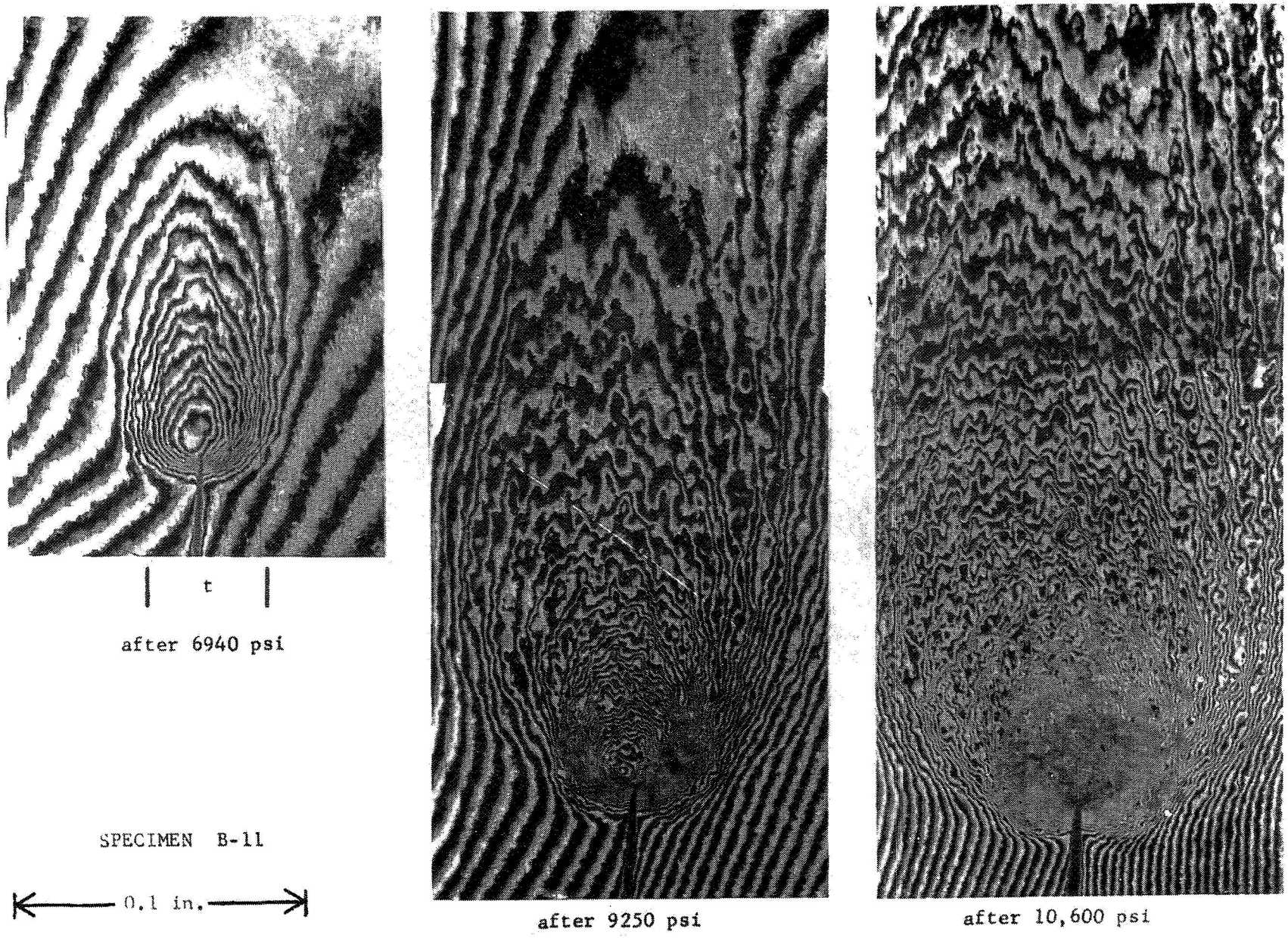

Figure 6. Interference Photographs, 70-30 Brass

Detailed strain distribution data from brass and aluminum specimens of various thicknesses are shown in Figures 7 through 12. As mentioned above the experimental results are obtained from moiré and interference photographs of the specimen and therefore derive from surface measurements. The strain values reported are considered to represent uniform strain within the sample only in the area more than about one thickness ahead of the crack and only when the deformation zone is large relative to t. Data outside these limits have been shown for comparison with those results considered valid. Analytical results corresponding to the specific specimen geometry, material properties and loading are also shown. A discussion of the analytical results and their comparison with experimental data is included in the next section.

Figures 7 and 8 are logarithmic plots of y direction strain distributions corresponding to samples of 90-10 and 70-30 brass respectively. In this and subsequent data the experimental loads were prearranged to produce about the same gross applied stress levels in specimens of the same materials. Thus any differences in the data for any given material can be attributed to thickness effect. For both the brasses the main difference noted is the slope of the experimental data near the crack tip. In both cases the thicker sample shows a lower negative slope and lower values of strain. These effects are attributed to thickness-direction constraint by the unyielded material behind the crack on the plastic deformation ahead of the crack. The constraint would be expected to be greater for thick samples, and also for low load data in a given sample since the deformed area is smaller relative to thickness at lower loads.

Figure 9 shows z direction results from 90-10 brass specimens for two of the same loads as the results in Figure 7. Here, however, strain data

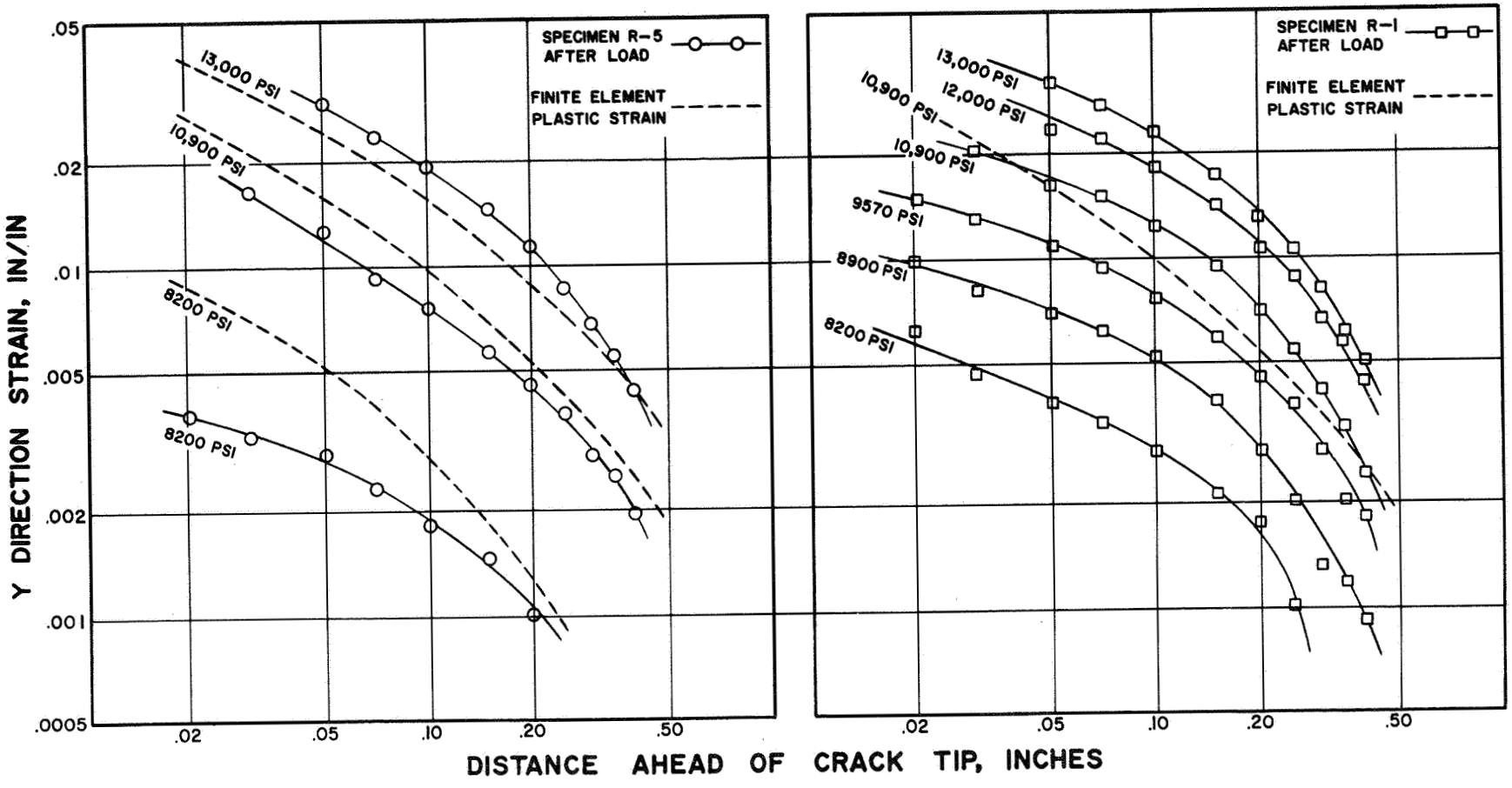

Figure 7. Measured and Calculated Strain, 90-10 Brass

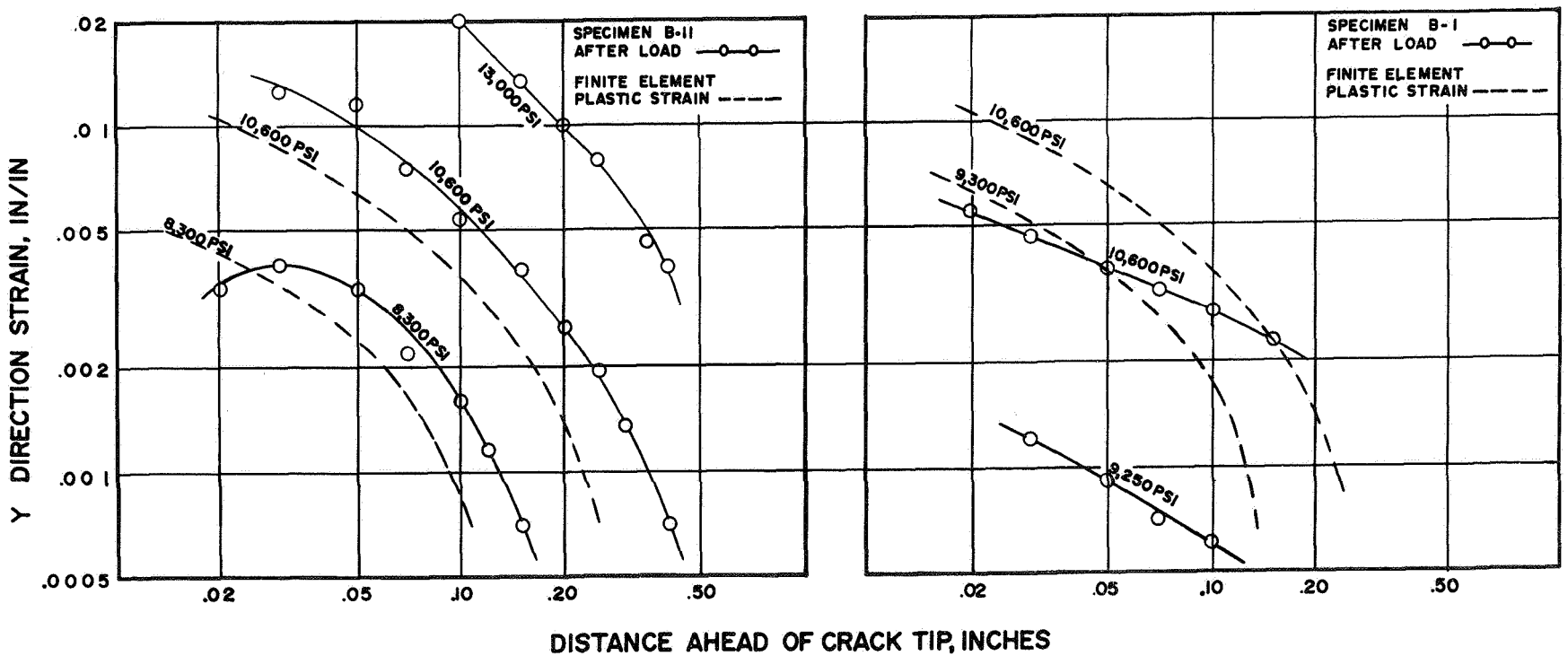

Figure 8. Measured and Calculated Strain, 70-30 Brass

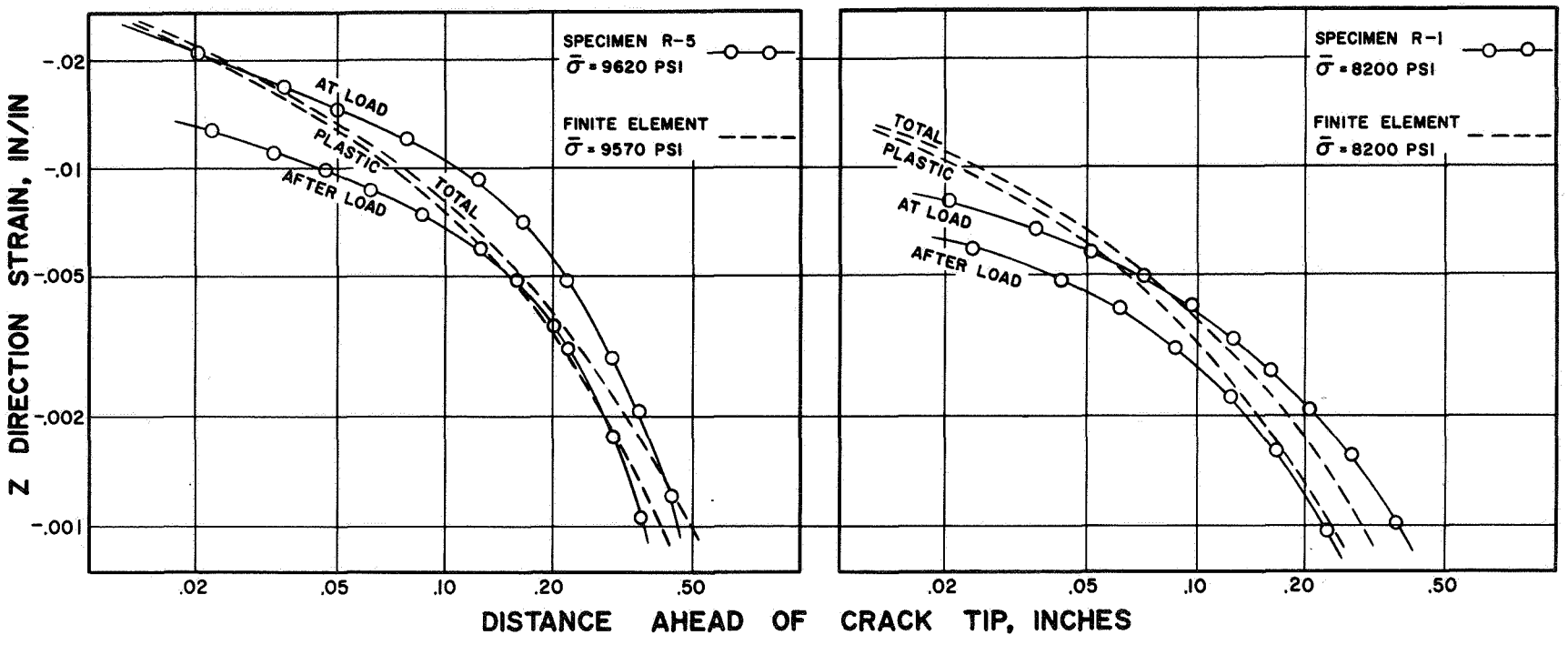

Figure 9. Measured and Calculated Strain, 90-10 Brass

are shown which correspond to both at-load and after-load conditions. The difference between the analytical data for the two loading conditions, i.e., total strain at load and plastic component of strain at load, is approximated by the ratio of gross applied stress to elastic modulus, $\Delta\epsilon = \bar{\sigma}/E$. The difference in the experimental data is much greater. This could be explained in part by reverse plastic deformation which is believed to occur in the experiment upon unloading, but is not included in the analysis. We are planning further experimental and analytical work which focuses on the unloading phenomenon. The after load z data represent most of our results in that the shape and magnitude of the z strain distributions are similar to those of the y strain distributions (compare Figures 7 and 9).

A field plot of after-load z direction strain from experiment and analysis is shown in Figure 10. The experimental data are shown as an interference photograph of specimen R-1 where the fringes also represent contours of constant strain. As mentioned above the experimental data near the crack tip may be affected by thickness constraint and also by the fact that the surface measurements do not always represent interior behavior.

The next two figures show results from 6061-T6 aluminum; Figure 11 compares experimental data from aluminum with 90-10 brass data, Figure 12 shows experimental and analytical data from two aluminum samples of different thickness. The experimental data from aluminum are quite different from the brass, showing a faster drop off of strain away from the crack and a peak followed by a drop off near the crack. Both effects can be explained by the increased tendency toward shear deformation in the aluminum. The shear mode results in a more contained deformation zone so a faster drop off away from the crack is expected. Near the crack the deformation is

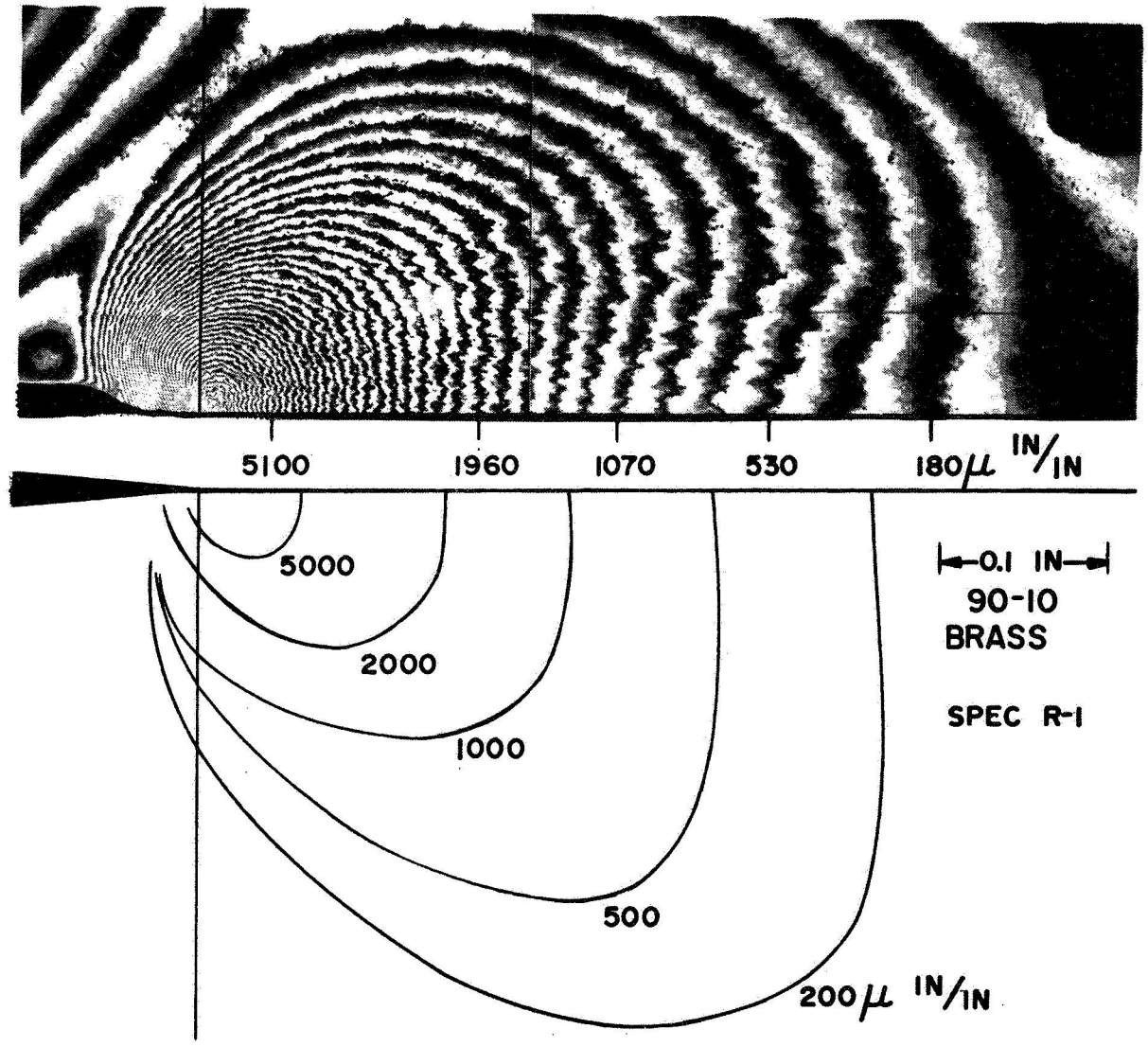

Figure 10. Measured and Calculated Strain Field Plot

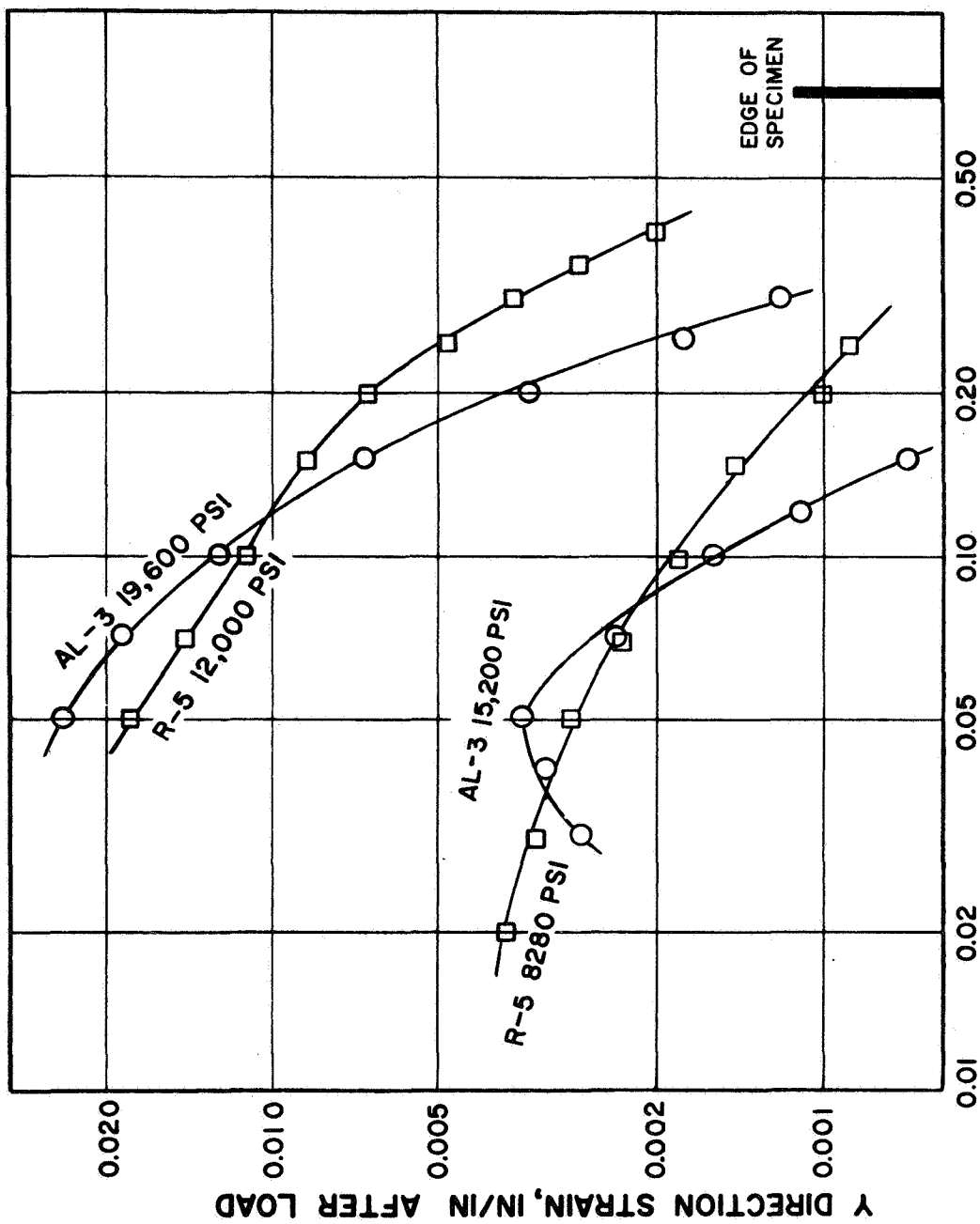

Figure 11. Measured Strain, 90-10 Brass and 6061-T6 Aluminum

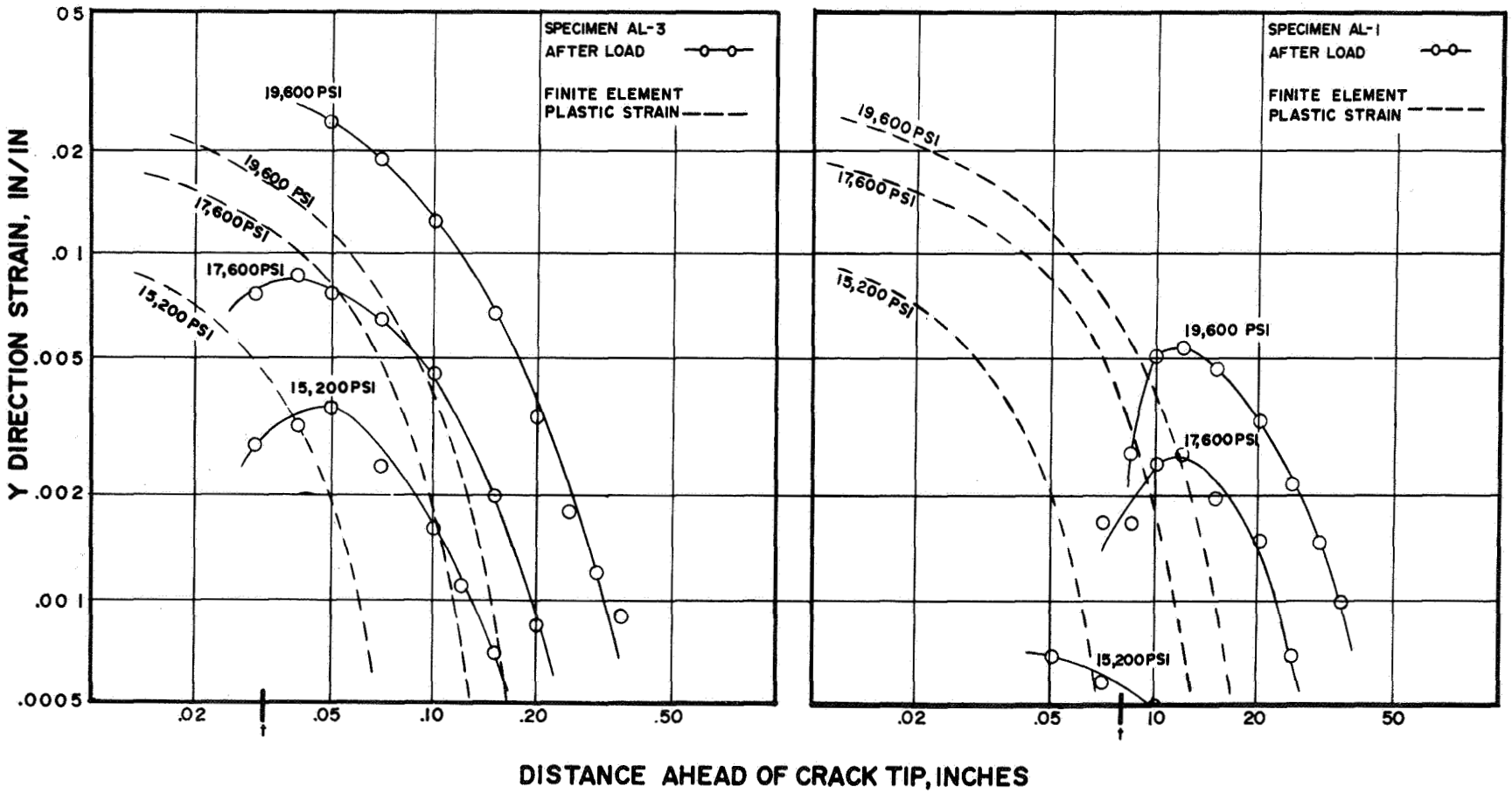

Figure 12. Measured and Calculated Strain, 6061-T6 Aluminum

concentrated on the shear planes above and below the crack so a lower strain is measured directly ahead of the crack.

Figure 13 shows an interference photo and an oblique lighting photo of aluminum specimen Al-3. Both photos show a shaded area near the crack-tip which indicates that the deformation is concentrated on the shear planes. The interference photo shows that away from the crack the deformation pattern spreads and becomes in-plane in nature. Also shown is a photo of specimen Al-1, the only specimen that fractured before gross yielding, taken after fracture with the specimen pieced together. On the surface, the fracture appears to proceed along one of the shear planes. From Figure 14 it is apparent that the internal fracture of specimen Al-1 is in fact a 45° shear type fracture. Thus, in this specimen fracture occurs by a shear process which is similar to the prior crack-tip deformation in the area near the crack.

INFORMATION FROM ANALYSIS

In view of the two-dimensional character of the analysis and the obviously three-dimensional nature of the deformation patterns observed in the 1018 steel, we would not anticipate useful comparisons for this material. Instead, attention was focused on the two brasses and the 6061-T6 aluminum.

The basis for comparison was selected to be the distribution of strains along the x-axis corresponding to the experimental measurements discussed above. Such a basis is sensitive to the overall performance of the analytical procedures. In order to compute strain at a given position, at a particular load, and for a specified geometry and material, all the basic elements of the theory are involved.*

*In contrast, one might consider an essentially kinematic comparison. An example would be crack opening at a given deflection of a three-point bend specimen.

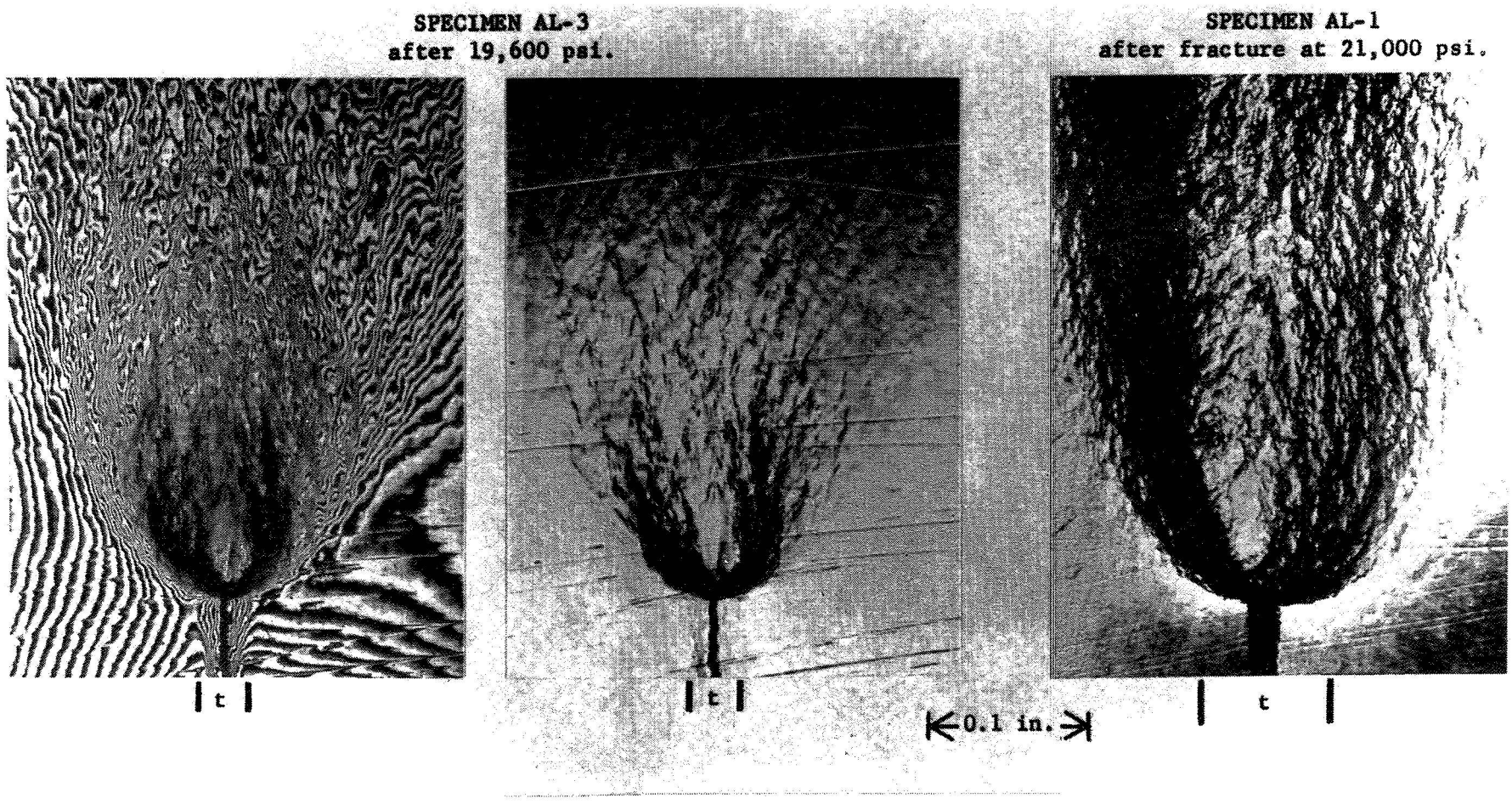

Figure 13. Interference and Oblique Light Photographs, 6061-T6 Aluminum

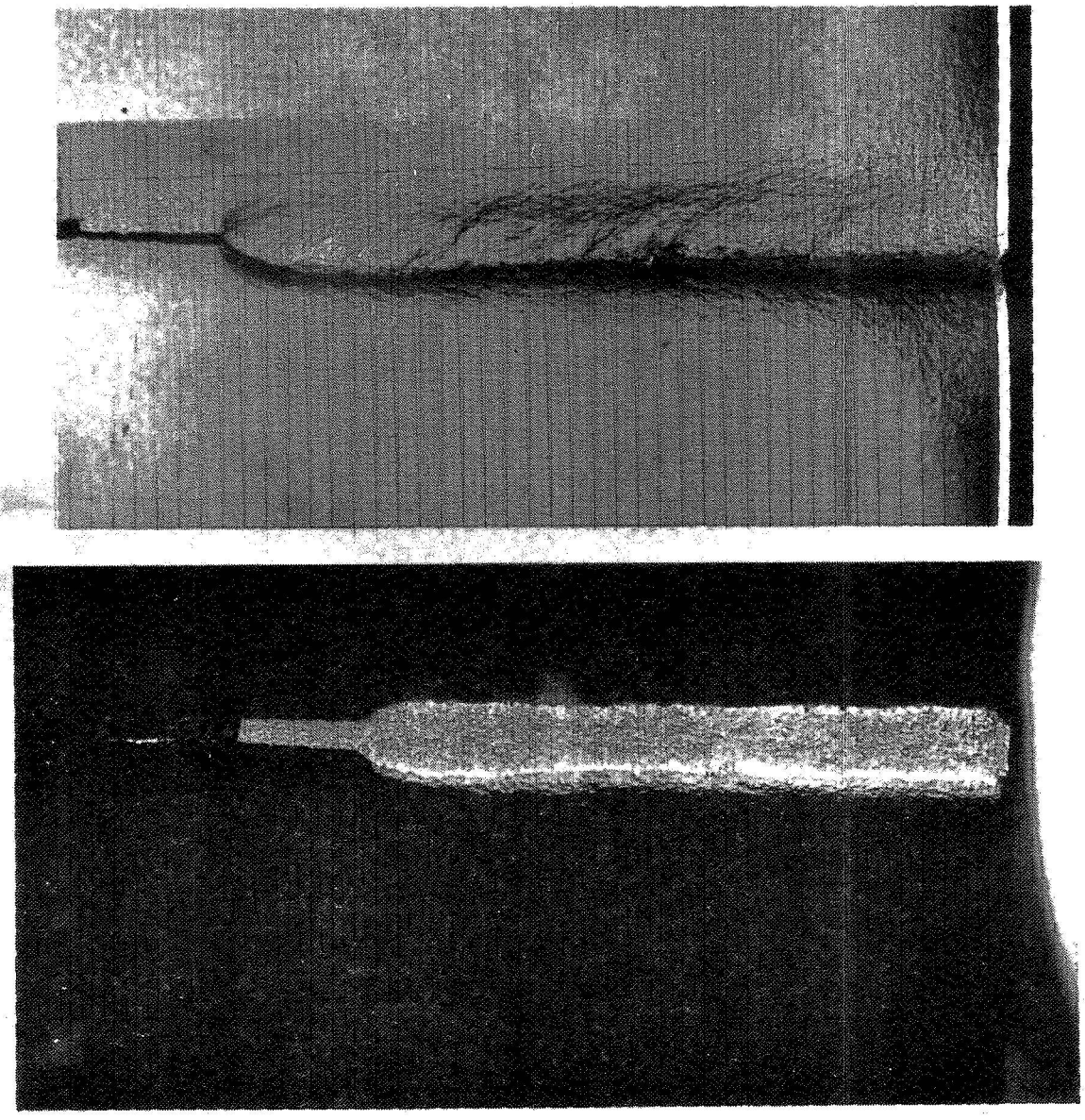

Figure 14. Fracture Appearance, 6061-T6 Aluminum, Specimen AL-1

Experimentally, such strains are obtained "at load" and "after load", the latter representing primarily the non-recoverable portion of the total strains. Analytically, one has both the total strains at load and their plastic components. The computer study was not set to unload the specimen for these cases. We believe it to be nonetheless reasonable to compare experimental and analytical results under two conditions. The first is at load; the second is after load (experimental) and the plastic components of the at-load strains (analytical).

Such comparisons are shown in Figures 7-10 and 12 for the two brasses and the aluminum. Examination of these data, as well as other results not presented, indicates that the comparisons are reasonable although not perfect. The discrepancies that do occur may be the result of several factors. First, there are some respects in which the physical specimen and the mathematical model do not correspond. For example, measurements are of surface behavior whereas the analysis concerns thickness-averaged quantities; also the actual mode of yielding does not of necessity correspond to the Mises criterion. Second, the assumption of plane stress is violated experimentally within about one plate thickness of the crack tip. It may be observed that the comparisons are at their worst at low loads when the extent of yielding is comparable to plate thickness and a significant transverse constraint must surely develop. Third, previous experience[1][2][3] suggests that the stress-strain curve may not adequately represent actual material behavior at initial yielding around the crack. This could result from the annealing process not fully removing the effects of fatiguing which would in turn cause poor comparisons at low load.

In any case, we are encouraged by the overall quality of the comparisons. Of particular interest is the slope of the logarithmic plot of strain versus distance since it is a good overall indication of both experimental and analytical data. The exponent m in the expression :

$$(\epsilon_y)_{plastic} = \text{const.}\ (x - b)^m$$

serves both to measure this slope and to summarize the data. We have determined this exponent from high load data at 0.1 inch ahead of the crack tip. These values are shown in Table II along with values predicted by Hutchinson[7] in another analysis. In that analysis the results include effects of work hardening and exclude the elastic component of strain,

TABLE II. SLOPES OF (Y) STRAIN DISTRIBUTION

	EXPERIMENTAL "t"	EXPERIMENTAL "m"	NUMERICAL "m"	ANALYTICAL Hutchinson "m"
PURE COPPER	.114	- .73	- .81	-.85
	.055	- .77		
90-10 BRASS	.118	- .57	- .75	-.86
	.036	- .67		
70-30 BRASS	.123	- .43	- .99	-.99
	.040	- .98		
6061-T6 ALUMINUM	.052	-1.18	-1.10	-.96
	.032	-1.28		

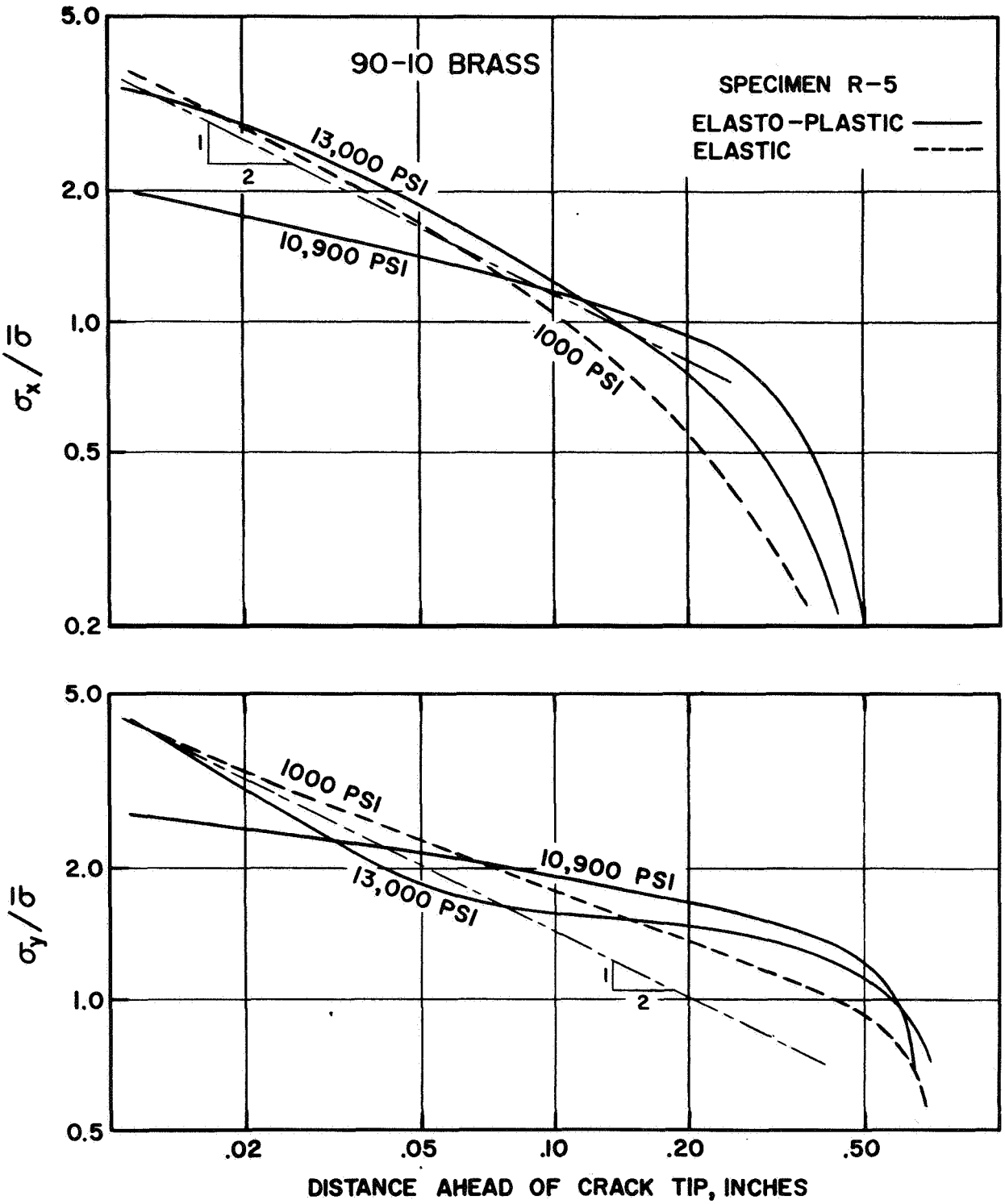

Figure 15. Calculated Stress Distributions, 90-10 Brass

but they are restricted to small scale yielding. Thus, one might expect that, although the analytical predictions follow the trend of the experiments, the numerical results are a better representation of the physical observations. It is also clear that measurements from thinner specimens correlate better with the numerical results.

Finally, we include some data from the numerical analysis showing stress distributions along the x axis. In Figure 15 are shown the $\sigma_x/\bar{\sigma}$ and $\sigma_y/\bar{\sigma}$ distributions corresponding to specimen R-5 for $\bar{\sigma}$ = 1000 (no yielding), 10,900 and 13,000 psi. Also shown is a line of slope = - 1/2 for reference. From these and other data it is clear that the steep elastic stress gradient is first attenuated as yielding progresses, as would be expected. Eventually there comes a point at which the stress concentration near the crack tip is regenerated, achieving the original level. Such behavior can be better seen in Figure 16 where stress concentration just ahead of the crack is plotted against applied stress. The initial sharp reduction mentioned above and reported previously[5] is evident; also seen is the increase in stress concentration at higher loads. It appears likely that this reconcentration is a result of growing strains in the vicinity of the crack tip. Since the material is forced to follow the stress-strain curve, the strain increase leads to stress reconcentration. The connection, of course, is not direct because only octahedral (or equivalent) quantities follow the curve, whereas the data are presented in terms of highly directional components. Still, the qualitative behavior may be traced to provide a clearer picture of yielding near a crack tip.

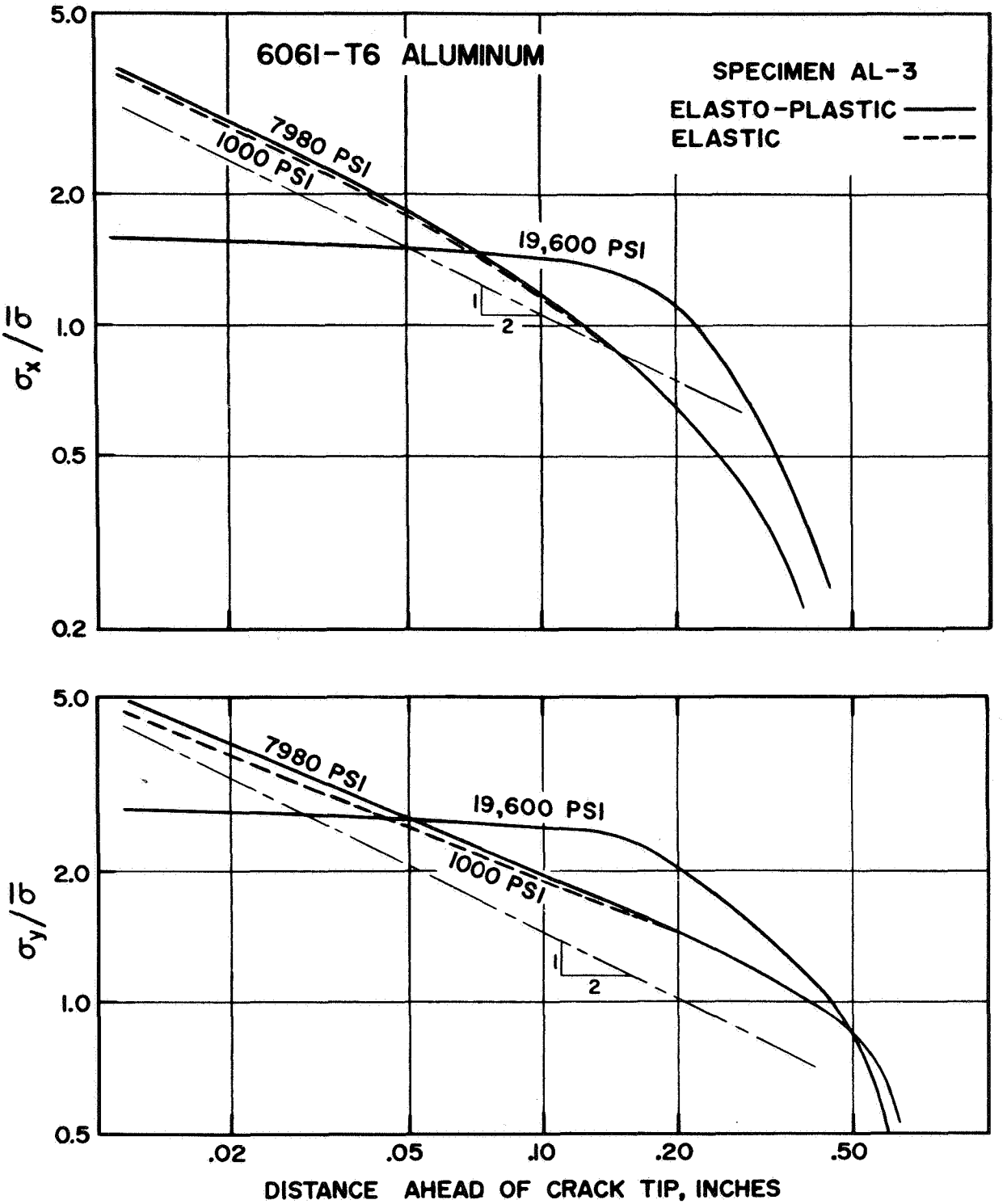

Figure 16. Calculated Stress Distributions, 6061-T6 Aluminum

Related results are shown for Al-3 in Figures 17 and 18. Comparison of Figures 16 and 18 shows that the analysis for Al-3 extended about one half as far as that for R-5 if it is permissible to scale such data on the basis of proportional limit.*

As might be anticipated, the stress gradient ahead of the crack tip is sharpened slight at $\bar{\sigma} = 7980$ psi, the load which corresponds to the peak in Figure 18. No similar load, i.e., corresponding to very early yielding, was shown for the brass. As yielding progresses, there is a reduction in both the gradient and the stress concentration as was seen with the brass. Indeed, Figure 17 suggests that there is almost no stress gradient ahead of the crack in the aluminum at the higher load. For the most part, this sort of behavior is explicable in terms of stress concentration reduction through yielding and a simple force balance across the net specimen width. No stress re-concentration is observed in the aluminum specimen, probably due to the lower applied stress (relative to proportional limit) and the lower strain hardening exponent.

CONCLUDING REMARKS

The work reported above is by no means considered to be conclusive; the final word in this area has certainly not been written. Rather, we are describing progress of our own efforts to provide positive interaction between theory and experiment. At this stage, we are confident that a reasonable basis for comparing results from the two sources can be established. The comparisons obtained thus far are encouraging in many respects. In general, the data follow similar and understandable trends. Such differences as do

---

*Alternatively one might use other measures of departure from elasticity such as an offset yield stress. The proportional limit is used here because it is a quantity more appropriate to the analysis.

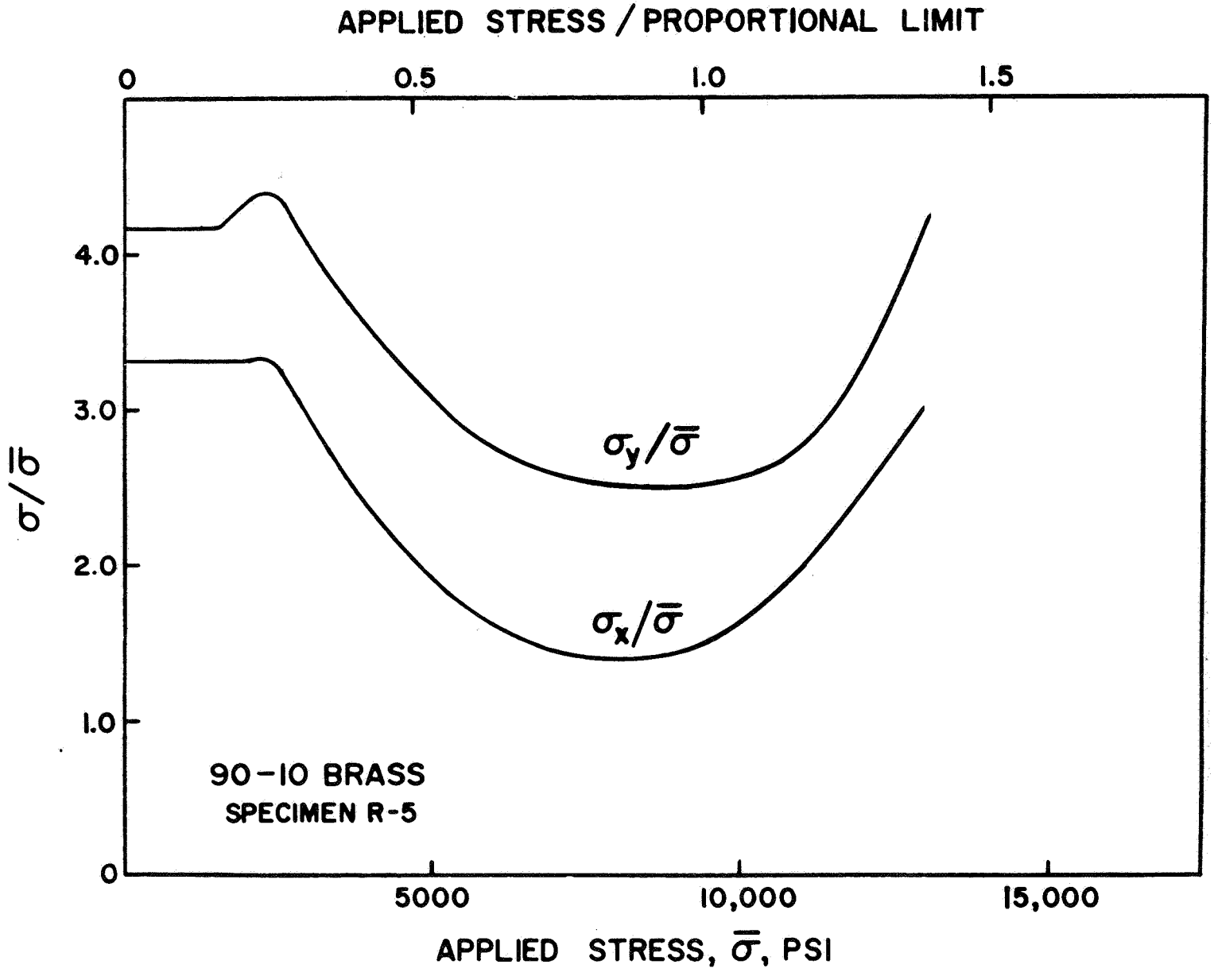

Figure 17. Calculated Stress Concentration, 90-10 Brass

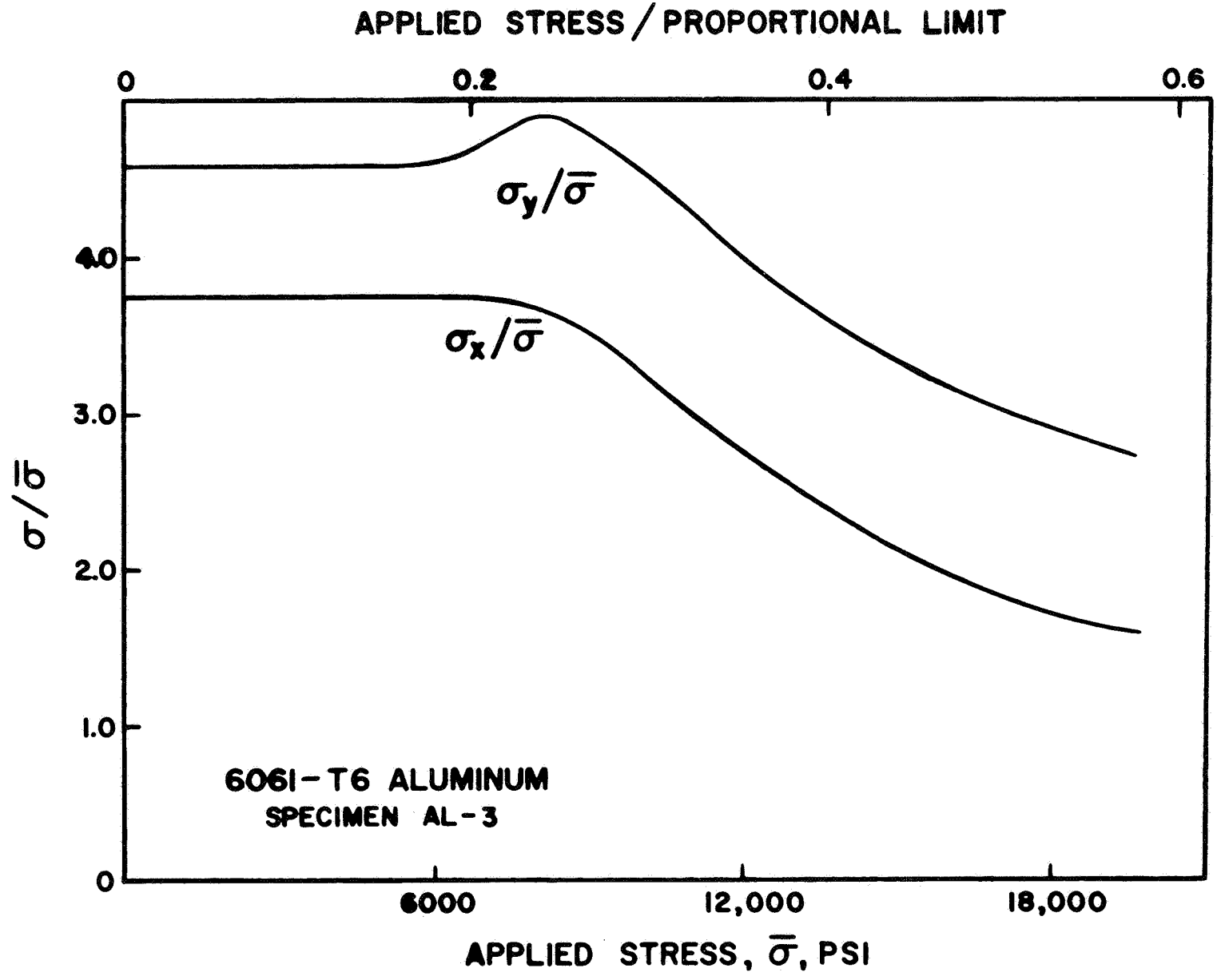

Figure 18. Calculated Stress Concentration, 6061-T6 Aluminum

occur remain to be investigated, and the requisite research seems to require attention to two main points. The first is a more accurate characterization of the material properties, both in the experimental measurement and in the manner in which the properties are included in the analysis. The second is increased accuracy and resolution of the theoretical and experimental methods.

One further point we would like to emphasize is the problem of comparing analytical results from a two-dimensional model with results from experiment which must be obtained from a three-dimensional specimen. The results presented herein clearly indicate that such three-dimensional aspects as thickness constraint and through-thickness shear deformation cannot be ignored. However, the results do indicate that in some cases the thickness effects are small.

ACKNOWLEDGMENT

J. L. Swedlow appreciates the support of the National Aeronautics and Space Administration through Research Grant NGR-39-002-023.

J. H. Underwood and D. P. Kendall appreciate the help of W. M. Yaiser in conducting the experiments reported in this paper.

REFERENCES

1. J. H. Underwood and D. P. Kendall, "Measurement of the Strain Distribution in the Region of a Crack Tip", presented before ASTM Committee E-24, March 1967

2. J. H. Underwood and D. P. Kendall, "Measurement of Microscopic Flastic Strain Distributions in the Region of a Crack Tip", Experimental Mechanics, Vol. 9, No. 7 (July 1969)

3. J. L. Swedlow, "Initial Comparison Between Experiment and Theory of the Strain Fields in a Cracked Copper Plate", Int. J. of Fract. Mech., Vol. 5, No. 1 (March 1969)

4. J. L. Swedlow, "Character of the Equations of Elasto-Plastic Flow in Three Independent Variables", Int. J. Non-Lin. Mech., Vol. 3, September 1968, pp. 325-336

5. J. L. Swedlow, M. L. Williams and W. H. Yang, "Elasto-Plastic Stresses and Strains in Cracked Plates", Proceedings of the First International Conference on Fracture, 1, pp. 259-282, 1965

6. W. W. Gerberich, "Plastic Strains and Energy Density in Cracked Plates, Part I - Experimental Technique and Results", Experimental Mechanics, Vol. 4, No. 11 (Nov. 1964)

7. J. W. Hutchinson, "Plastic Stress and Strain Fields at a Crack Tip", J. Mech. Phys. Solids, 1968, Vol. 16, pp. 337-347

Unclassified
Security Classification

DOCUMENT CONTROL DATA - R & D

(Security classification of title, body of abstract and indexing annotation must be entered when the overall report is classified)

1. ORIGINATING ACTIVITY *(Corporate author)*

Watervliet Arsenal
Watervliet, N.Y. 12189

2a. REPORT SECURITY CLASSIFICATION

Unclassified

2b. GROUP

3. REPORT TITLE

EXPERIMENTAL AND ANALYTICAL STRAINS IN AN EDGE-CRACKED SHEET

4. DESCRIPTIVE NOTES *(Type of report and inclusive dates)*

Technical Report

5. AUTHOR(S) *(First name, middle initial, last name)*

John H. Underwood
J. L. Swedlow
David P. Kendall

6. REPORT DATE	7a. TOTAL NO. OF PAGES	7b. NO. OF REFS
September 1969	38	7

8a. CONTRACT OR GRANT NO.	9a. ORIGINATOR'S REPORT NUMBER(S)
AMCMS No. 5011.11.85500	
b. PROJECT NO. DA Project 1-T-0-61102-B32A	WVT-6933
c.	9b. OTHER REPORT NO(S) *(Any other numbers that may be assigned this report)*
d.	

10. DISTRIBUTION STATEMENT

This document has been approved for public release and sale; its distribution is unlimited.

11. SUPPLEMENTARY NOTES	12. SPONSORING MILITARY ACTIVITY
	U. S. Army Weapons Command

13. ABSTRACT

The nature and some details of the elasto-plastic strain distribution ahead of the crack tip in an edge-cracked sheet has been determined by experiment and analysis. The experiment uses the optical interference and moire techniques. The analysis is a generalized plane stress model using the finite element method; the measured uniaxial stress-strain properties of the materials are used as input to the analysis. Materials investigated by one or both methods are 1018 steel, copper, 90-10 and 70-30 brass, and 6061-T6 aluminum. Of these materials, meaningful comparisons between experiment and analysis have been made for those with no discontinuity in uniaxial behavior; copper, 90-10 brass, and aluminum. The agreement between experiment and analysis can be significantly affected by how well the early, uniaxial, yield properties used in the analysis represent the actual properties of the experimental specimens.

The main factors which control the general nature of crack-tip strain are (1) degree of strain hardening, shown by both experimental and analytical results and (2) thickness of the experimental specimen. For materials of low strain hardening and at relatively low loads, the measured crack-tip deformation tends to be three dimensional in character and restricted in extent to about one specimen thickness in the direction normal to the crack. For higher hardening and at higher loads, broader, two-dimensional strain distributions result with better correlation with analysis. Stress distributions from the analysis in the area ahead of the crack are also shown and tend to support the strain results.

DD FORM 1 NOV 68 1473 REPLACES DD FORM 1473, 1 JAN 64, WHICH IS OBSOLETE FOR ARMY USE.

Unclassified
Security Classification

14. KEY WORDS	LINK A		LINK B		LINK C	
	ROLE	WT	ROLE	WT	ROLE	WT
Crack-tip Strain						
Fracture Mechanics						
Finite Elements						
Optical Measurement						
Strain Distribution						
Strain Hardening						